[1]Vidyashree K.

[2]Sharanagouda Malipatil

[3]Mahantesh S. Swamy

Darcy-Benard-Oldroyd Convection in a Rotating Porous Layer with an Internal Heat Source

JES Journal of Electrical Systems

Abstract: - This research examines the stability of an Oldroyd-B fluid within a horizontal porous layer, influenced by both an internal heat source and rotation. The energy equation incorporates a term for internal heat generation, and a modified Darcy-Oldroyd model that includes the Coriolis effect is used to describe momentum. To explore the impact of rotation, internal heat generation, and viscoelasticity on system stability, a linear stability analysis is performed. For nonlinear stability analysis, the normal mode method is combined with the Galerkin method of weighted residuals and the truncated Fourier series method. The Runge-Kutta-Gill technique is then applied to numerically solve the resulting system of nonlinear differential equations. The study investigates how various controlling parameters affect stability and convective heat transfer. It is observed that the initial conduction state transitions into convective motion. Key factors in initiating convection include the internal heat production coefficient and the stress-relaxation parameter. Conversely, rotation, the strain-retardation coefficient, and the heat-capacity ratio delay the onset of convection. The Vadasz number exhibits two distinct effects.

Keywords: Darcy model, Oldroyd-B model, viscoelastic fluid, thermal convection, internal heat generation, Rayleigh number, Nusselt number, heat transfer.

Nomenclature

Da	Darcy number, K/d^2
$\mathbf{g}$	acceleration due to gravity (m/s²)
k	horizontal wavenumber (m⁻¹)
K	permeability (m²)
Nu	Nusselt number
Pr	Prandtl number, $\mu/\rho_0\kappa$
$\mathbf{v}$	velocity vector (m/s)
Q_I	internal heat generation (W/m³)
Ra_D	Darcy-Rayleigh number, $\rho_o\alpha g\Delta TdK/\mu\kappa$
Ra_I	internal Rayleigh number, Qd^2/κ
t	time (s)
Ta	Taylor number, $\left(2\Omega K/\varepsilon\kappa\right)^2$
Va	Darcy-Prandtl number, $\varepsilon Pr/Da$
α	thermal expansion coefficient (K⁻¹)
γ	ratio of heat capacities, $(\rho c)_m/(\rho c)_f$
ε	porosity
κ	thermal diffusivity (m²/s)
λ_1	Deborah number, $\overline{\lambda}_1\kappa/d^2$

[1] Department of Mathematics, Sharnbasva University, Kalaburagi, India

[2] Department of Mathematics, Poojya Doddappa Appa College of Engineering, India

[3]Department of Mathematics, Government College (Autonomous), Kalaburagi, India.

* Corresponding author: E-mail: mssmaths@gmail.com

Copyright © JES 2024 on-line : journal.esrgroups.org

λ_2 strain-retardation parameter, $\overline{\lambda_2}\kappa/d^2$

μ dynamic viscosity (kg/(m·s))

ρ density (kg/m³)

ω temporal growth rate (s^{-1})

$\mathbf{\Omega}$ angular velocity, $(0, 0, \Omega)$, (rad/s)

ψ stream function (m^2/s)

*E-mail: mssmaths@gmail.com

1. INTRODUCTION

Geothermal energy, the petroleum industry, and thermal insulation are just a few of the many real-world applications of thermal convection in porous media. Researchers such as Ingham and Pop [1, 2], Nield and Bejan [3], Vafai [4], and Vadasz [5] have made significant contributions that have advanced the field. From a rheological standpoint, understanding the viscoelastic nature of the asthenosphere and mantle is crucial (Lowrie [6]). Studies show that viscoelastic liquids are involved in numerous processes, including snow formation and food delivery. Unlike Rayleigh-Benard convection in Newtonian fluids, the study of convection in viscoelastic fluids is still emerging (Li and Khayat [7]).

In polymeric liquids with coagulated viscosity, flow and turbulence are consistent, unlike in Newtonian fluids. The inherent elasticity of these fluids is expected to cause oscillatory convection. Elasticity introduces instability, whereas porosity influences stability, as noted by Kim et al. [8]. The oscillatory mode is considered effective for studying convection since it simplifies to elasticity-independent supercritical and stable bifurcation forms. However, research on oscillatory convection in viscoelastic fluids is limited, and even less is known about related challenges in porous media. Researchers like O'Connell and Budiansky [9], Griffiths [10], Rudraiah et al. [11], Yoon et al. [12], Malashetty et al. [13], and Swamy et al. [14] have explored thermal convection in viscoelastic fluids.

Several scientists have examined the effects of rotation on convection in porous media, including Friedrich [15], Patil [16], Vaidyanathan [17], Palm [18], Jou [19], Qin [20], Straughan [21], Govender [22], Malashetty [23-25], Malashetty et al. [26, 27], Capone [28], and Enagi [29]. This research is highly relevant to chemical processes, alloy solidification and centrifugation, spinning equipment, and the fuel industry.

Thermal convection in a porous layer with internal heat production can be used to evaluate heat removal in particulate nuclear fuel debris from potential reactor accidents. Natural or radioactive heating due to nuclear wastes is also studied in subsurface porous layers. Internal heating is crucial in reactors with exothermic reactions, as it creates a nonlinear temperature gradient, allowing convection even with a minimal temperature difference between surfaces. Thus, internal heat production primarily controls convection onset in the porous layer. Many researchers have focused on this topic, including Thirlby [30], Ahmed and Rashed [31], Mahabaleshwar et al. [32], Baitharu et al. [33], Yadav et al. [34], Sahoo et al. [35], and Enagi et al. [29].

The impact of rotation and internal heat sources on the thermal analysis of an Oldroyd-B fluid in a densely packed porous material is seldom studied. There is still much to explore and questions to answer in this field. This investigation aims to clarify the roles of viscoelastic factors, the internal heat production coefficient, and the angular velocity of rotation in determining the onset threshold of thermal convection. Another goal is to understand how these variables affect heat transfer through the porous layer.

2. MATHEMATICAL FORMULATION

The problem involves an infinite horizontal porous layer filled with an Oldroyd-B liquid, bounded by two parallel surfaces at z=0z = 0z=0 and z=hz = hz=h. These surfaces are considered stress-free and isothermal. The porous layer rotates uniformly around the z-axis with an angular velocity Ω\OmegaΩ, while the gravitational force ggg acts downward. A thermal gradient ΔT\Delta TΔT is established between the two surfaces by uniformly heating the lower surface. Additionally, internal heat generation is taken into account in the system. The governing equations for this problem, under the Boussinesq approximation, are as follows:

$$\nabla \cdot \mathbf{v} = 0 \qquad (1)$$

The Cauchy stress tensor τ'_{ij} is given by

$$\tau'_{ij} = -p\delta_{ij} + \tau_{ij}\,, \qquad (2)$$

where τ_{ij} is the shear-stress tensor which is related to the strain-rate tensor e_{ij} through Oldroyd-B constitutive relation

$$\left(1+\overline{\lambda}_1 \frac{D}{Dt}\right)\tau_{ij} = \mu\left(1+\overline{\lambda}_2 \frac{D}{Dt}\right)e_{ij}\,. \qquad (3)$$

with $e_{ij} = \nabla\mathbf{v} + \nabla\mathbf{v}^T$ and $\frac{D}{Dt}(\mathbf{A}) = \left(\frac{\partial}{\partial t} + \mathbf{v}\cdot\nabla\right)\mathbf{A} - \mathbf{A}(\nabla\mathbf{v}) - (\nabla\mathbf{v})^T\,\mathbf{A}$.

The Darcy's law $\nabla p = -\frac{\mu}{K}\mathbf{v}_D$ is modified for the viscoelastic liquid as

$$\left(1+\overline{\lambda}_1 \frac{\partial}{\partial t}\right)\nabla p = -\frac{\mu}{K}\left(1+\overline{\lambda}_2 \frac{\partial}{\partial t}\right)\mathbf{v}_D\,. \qquad (4)$$

The expression $\mathbf{v}_D = \varepsilon\mathbf{v}$, ($\varepsilon$ being the porosity) determines the relationship between the seepage velocity and the usual velocity. Under the consideration of the balance of forces, the law of conservation of linear momentum can now be written as

$$\rho_0\left(\frac{\partial\mathbf{v}}{\partial t} + (\mathbf{v}\cdot\nabla)\mathbf{v}\right) + 2(\boldsymbol{\Omega}\times\mathbf{v}) = -\nabla p + \rho\mathbf{g} + \mathbf{r} + \nabla\cdot\tau_{ij}\,, \qquad (5)$$

where $\mathbf{r}$ is the Darcy resistance, Eq (4) gives the amount of resistance to the flow of fluid through the porous medium, $\mathbf{r}$ which can therefore be inferred to satisfy (4).

$$\left(1+\overline{\lambda}_1 \frac{\partial}{\partial t}\right)\mathbf{r} = -\frac{\mu}{K}\left(1+\overline{\lambda}_2 \frac{\partial}{\partial t}\right)\mathbf{v}_D\,. \qquad (6)$$

Using (6) in (5) one can obtain

$$\left(1+\overline{\lambda}_1 \frac{\partial}{\partial t}\right)\left(\rho_0\left(\frac{\partial\mathbf{v}}{\partial t} + (\mathbf{v}\cdot\nabla)\mathbf{v}\right) + 2(\boldsymbol{\Omega}\times\mathbf{v}) + \nabla p - \rho\mathbf{g} - \nabla\cdot\tau_{ij}\right) = -\frac{\mu}{K}\left(1+\overline{\lambda}_2 \frac{\partial}{\partial t}\right)\mathbf{v}_D$$

One can ignore $(\mathbf{v}\cdot\nabla)\mathbf{v}$ and $\nabla\cdot\tau_{ij}$ for Darcy's model and use $\mathbf{v} = \mathbf{v}_D/\varepsilon$, so that

$$\left(1+\overline{\lambda}_1 \frac{\partial}{\partial t}\right)\left(\frac{\rho_0}{\varepsilon}\frac{\partial\mathbf{v}}{\partial t} + \frac{2}{\varepsilon}(\boldsymbol{\Omega}\times\mathbf{v}) + \nabla p - \rho\mathbf{g}\right) = -\frac{\mu}{K}\left(1+\overline{\lambda}_2 \frac{\partial}{\partial t}\right)\mathbf{v} \qquad (7)$$

The heat-transport equation, by assuming the equilibrium among solid and liquid phases, is

$$(\rho c)_m \frac{\partial T}{\partial t} + (\rho c)_f (\mathbf{v}\cdot\nabla)T = (\rho c)_m \kappa\nabla^2 T + (\rho c)_m Q_I (T - T_0) \qquad (8)$$

where $(\rho c)_m = \varepsilon(\rho c)_f + (1-\varepsilon)(\rho c)_s$ denotes the specific heat of the porous medium $(\rho c)_f$ and $(\rho c)_s$ being heat-capacities of liquid and solid phases respectively, Q_I quantifies the amount of heat generation within the bulk of the porous layer and $\nabla^2 = \partial^2/\partial x^2 + \partial^2/\partial y^2 + \partial^2/\partial z^2$ designates the Laplacian operator. The equation of state is

$$\rho = \rho_0 \left(1-\alpha\left(T-T_0\right)\right) \tag{9}$$

Fluid is at rest in a basic state and the density, pressure and temperature are given by

$$\rho_b(z) = \rho_0 \left(1-\alpha\,\Delta T\left(\sin\left(\sqrt{Q_I/\kappa}\,h\left(1-z/h\right)\right)\Big/\sin\left(\sqrt{Q_I/\kappa}\,h\right)\right)\right), \tag{10}$$

$$p_b(z) = \rho_0 \mathbf{g}\left(z-\left(\alpha\,\Delta T\Big/\sqrt{Q_I/\kappa}\right)\left(\cos\left(\sqrt{Q_I/\kappa}\,h\left(1-z/h\right)\right)\Big/\sin\left(\sqrt{Q_I/\kappa}\,h\right)\right)\right), \tag{11}$$

$$T_b(z) = T_0 + \Delta T\left(\sin\left(\sqrt{Q_I/\kappa}\,h\left(1-z/h\right)\right)\Big/\sin\left(\sqrt{Q_I/\kappa}\,h\right)\right), \tag{12}$$

The stability of the system is scrutinized by enforcing the perturbations on the basic state.

$$\mathbf{v} = \mathbf{v}',\ T = T_b(z)+T',\ p = p_b(z)+p',\ \rho = \rho_b(z)+\rho', \tag{13}$$

where this prime indicates the quantity in the perturbed state. We place (13) along with the basic solutions (10)-(12), in the governing equations (1), (7)-(9) and eliminate p'. Believe the flow to be two-dimensional and thus incorporate the stream function such that $(u', w') = (\partial/\partial z,\ -\partial/\partial x)\psi'$. We are yet to understand that the velocity component in the *y*-direction does not become extinct and hence opt v' to be V' and refer state it as the rotation-induced zonal velocity. We use $(x,z) = h\left(x^*,\ z^*\right),\ \ t = \left(h^2/\kappa\right)t^*,\ \ \psi = \kappa\psi^*,\ V' = \left(\kappa/d\right)V^*$, and $T' = \left(\Delta T\right)T^*$ express the equations in the non-dimensional form as displayed below

$$\left(\left(1+\lambda_1\frac{\partial}{\partial t}\right)\frac{1}{Va}\frac{\partial}{\partial t}+\left(1+\lambda_2\frac{\partial}{\partial t}\right)\right)\nabla^2\psi-\sqrt{Ta}\left(1+\lambda_1\frac{\partial}{\partial t}\right)\frac{\partial v}{\partial z}+Ra_D\left(1+\lambda_1\frac{\partial}{\partial t}\right)\frac{\partial T}{\partial x}=0 \tag{14}$$

$$\left(\frac{1}{Va}\left(1+\lambda_1\frac{\partial}{\partial t}\right)\frac{\partial}{\partial t}+\left(1+\lambda_2\frac{\partial}{\partial t}\right)\right)V+\sqrt{Ta}\left(1+\lambda_1\frac{\partial}{\partial t}\right)\frac{\partial\psi}{\partial z}=0, \tag{15}$$

$$\left(\gamma\frac{\partial}{\partial t}-\nabla^2-Ra_I\right)T-\frac{\partial(\psi,\,T)}{\partial(x,\,z)}+\frac{\sqrt{Ra_I}}{\sin\left(\sqrt{Ra_I}\right)}\cos\left(\sqrt{Ra_I}\,(1-z)\right)\frac{\partial\psi}{\partial x}=0, \tag{16}$$

Since bounding surfaces are presumed to be stress-free and isothermal,"

$$\psi = D^2\psi = \frac{\partial V}{\partial z} = T = 0 \text{ at } z = 0,\ 1. \tag{17}$$

3. LINEAR THEORY WITH GALERKIN TECHNIQUE

The non-linear terms in Eqs. (14)–(16) are ignored in the linear stability theory since the imposed perturbations are assumed to be minor. The normal mode analysis is then applied to the resultant eigenvalue issue. Consequently, periodic waveforms are postulated for the infinitesimally small disturbances.

$$\begin{pmatrix}\psi\\ T\\ V\end{pmatrix} = \begin{pmatrix}\Psi(z)\\ \Theta(z)\\ \Phi(z)\end{pmatrix}e^{i(\omega t+kx)}, \tag{18}$$

These periodic, tiny disturbances may either increase or diminish, depending on the growth rate ω. The following is what we get when we plug Eq. (18) into Eqs.(14-17)

$$\left(\frac{i\omega}{Va}\left(1+i\omega\lambda_1\right)+\left(1+i\omega\lambda_2\right)\right)\left(D^2-k^2\right)\Psi+ikRa_D\left(1+i\omega\lambda_1\right)\Theta-\sqrt{Ta}\left(1+i\omega\lambda_1\right)D\Phi=0 \tag{19}$$

$$\left(D^2-k^2-i\omega\gamma+Ra_I\right)\Theta-ik\,f(z)\Psi=0\,, \tag{20}$$

$$\left(\frac{i\omega}{Va}\left(1+i\omega\lambda_1\right)+\left(1+i\omega\lambda_2\right)\right)\Phi+\sqrt{Ta}\left(1+i\omega\lambda_1\right)D\Psi=0 \tag{21}$$

$$\Psi=D^2\Psi=\frac{\partial\Phi}{\partial z}=\Theta=0 \text{ at } z=0,\ 1\,. \tag{22}$$

where $f(z)=\left(\sqrt{Ra_I}\Big/\sin\left(\sqrt{Ra_I}\right)\right)\cos\left(\sqrt{Ra_I}\,(1-z)\right)$. According to the Galerkin method we choose

$$\begin{pmatrix}\Psi(z)\\ \Theta(z)\\ \Phi(z)\end{pmatrix}=\begin{pmatrix}A\Psi_1(z)\\ B\Theta_1(z)\\ C\Phi_1(z)\end{pmatrix}, \tag{23}$$

where A, B and C are constants and $\Psi_1(z)$, $\Theta_1(z)$, $\Phi_1(z)$ are so selected that they satisfy the boundary constraints (22). On multiplying Eq. (23), (24), (25) respectively by $\Psi_1(z)$, $\Theta_1(z)$, $\Phi_1(z)$ and integrating the resultant equations w.r.t z between the limits 0 and 1, we acquire

$$\left(\frac{i\omega}{Va}\left(1+i\omega\lambda_1\right)+\left(1+i\omega\lambda_2\right)\right)X_1A+ikRa_D\left(1+i\omega\lambda_1\right)X_2B-\sqrt{Ta}\left(1+i\omega\lambda_1\right)X_3C=0 \tag{24}$$

$$ik\,X_4A+\left(\left(i\omega\gamma-Ra_I\right)X_5-X_6\right)B=0\,, \tag{25}$$

$$\sqrt{Ta}\left(1+i\omega\lambda_1\right)X_7A+\left(\frac{i\omega}{Va}\left(1+i\omega\lambda_1\right)+\left(1+i\omega\lambda_2\right)\right)X_8C=0 \tag{26}$$

The Darcy-Rayleigh number may be expressed as follows, "given that equation (24)-(27) must have a non-trivial solution:

$$Ra_D=\frac{\left(\omega^2M_iN_i+M_rN_r\right)}{k^2X_2X_4X_8\left(M_r^2+\omega^2M_i^2\right)}+i\omega\frac{\left(M_rN_i-M_iN_r\right)}{k^2X_2X_4X_8\left(M_r^2+\omega^2M_i^2\right)}\,. \tag{27}$$

Since, $\omega=\omega_r+i\omega_i$, the case $\omega_r<0$ specifies a stable state while $\omega_r>0$ corresponding to the unstable mode. A neutral state is attained $\omega_r=0$. The steady-marginal stability can be observed for $\omega=0$ (i.e., $\omega_r=\omega_i=0$) with which Eq. (27) abridges to the expression of stationary Rayleigh number

$$Ra_D^{St}=\left(Ta\,X_3X_7+X_1X_8\right)\left(Ra_IX_5+X_6\right)\Big/k^2X_2X_4X_8\,. \tag{28}$$

The trial functions which satisfy the boundary conditions (22) are obviously,

$$\begin{pmatrix}\Psi_1(z)\\ \Theta_1(z)\\ \Phi_1(z)\end{pmatrix}=\begin{pmatrix}\sin(\pi z)\\ \sin(\pi z)\\ \cos(\pi z)\end{pmatrix}$$

Using these one can estimate X_i's and then implant into Eq. (28) to receive

$$Ra_D^{St}=\left(4\pi^2-Ra_I\right)\left(\delta^2-Ra_I\right)\left(\delta^2+\pi^2Ta\right)\Big/4\pi^2k^2\,, \tag{29}$$

where $\delta^2 = k^2 + \pi^2$ .Equation (29) is unconstrained to viscoelasticity, so it bears a resemblance to the one which is obtained for a viscous Newtonian fluid. The validity of our work can be ascertained through Table 1, wherein we recovered the previous classical results as a special case of Eq. (29).”

Special Case	**The result recovered from Eq. (29)**	**Previously published work**
$Ra_I = 0$	$\left(Ra_D^{St}\right)_{Ra_I=0} = \frac{\delta^2}{k^2}\left(\delta^2 + \pi^2 Ta\right)$	Palm and Tyvand [17]
$Ra_I = 0,\ Ta = 0$	$\left(Ra^{St}\right)_{Ra_I=0,Ta=0} = \frac{\delta^4}{k^2}$	Horton and Rogers [34] and Lapwood [35]

Table 1.Recovery of the previously published results

Now we move onto discuss the behaviour of Eq. (27) with the non-zero growth-rate *i.e.*, $\omega \neq 0$. As Ra_D portrays a physical phenomenon, it should not be imaginary and hence, Eq. (27) admits $\left(M_r N_i - M_i N_r\right) = 0$ as $\omega \neq 0$. This affords the expression for ω^2

$$B_0\left(\omega^2\right)^3 + B_1\left(\omega^2\right)^2 + B_2\left(\omega^2\right) + B_3 = 0\,. \qquad (30)$$

The real part of Eq. (27) then symbolizes the expression for the Oscillatory Rayleigh number

$$Ra_D^{Osc} = \frac{\left(\omega^2 M_i N_i + M_r N_r\right)}{k^2 X_2 X_4 X_8\left(M_r^2 + \omega^2 M_i^2\right)}\,. \qquad (31)$$

To estimate Ra_{Dc}^{Osc} , we minimize (31) w.r.t. *k*, after substituting $\omega^2\ (>0)$ from Eq. (30).

4. WEAK NON-LINEAR THEORY

It is recommended to use the weak non-linear theory for determining the convection amplitudes and the heat transfer coefficient. This method reduces the amount of mathematics required to grasp the physical process. It's an entry point towards understanding the complete nonlinearity of the issue. Given that the anticipated amplitude of the perturbations is finite, it makes sense to describe them as a restricted Fourier series.

$$\psi = A_{11}(t)\sin(kx)\sin(\pi z)\,, \qquad (32a)$$

$$T = B_{11}(t)\cos(kx)\sin(\pi z) + B_{02}(t)\sin(2\pi z)\,, \qquad (32b)$$

$$V = C_{11}(t)\sin(kx)\cos(\pi z) + C_{20}(t)\sin(2\pi x)\,. \qquad (32c)$$

The dynamics of the system must be analysed to determine the amplitudes A, B, C's that vary with time in unstable nonlinear convection. The following Lorenz system of autonomous nonlinear differential equations is obtained by substituting Eq. (32) into Eqs. (14-16) and comparing the coefficients of similar terms:

$$\frac{d\mathbf{X}}{dt} = \mathbf{D}\,, \qquad (33)$$

where $\mathbf{X} = (A_{11},\ C_{11},\ C_{20},\ G_1,\ G_2,\ G_3,\ B_{11},\ B_{02})^T$, $\mathbf{D} = (G_1,\ G_2,\ G_3,\ D_1,\ D_2,\ D_3,\ G_4,\ D_4)^T$

with $D_1 = -\frac{Va}{\delta^2}\left(\frac{1}{\lambda_1}\left(\left(\delta^2 A_{11} + \lambda_2 \delta^2 G_1\right) - \left(-\frac{\delta^2}{Va} G_1 + \sqrt{Ta}\,\pi C_{11} - Ra_D k B_{11}\right)\right) - \sqrt{Ta}\,\pi G_2 + Ra_D k G_4\right)$

$D_2 = -\frac{Va}{\lambda_1}\left(\left(C_{11} + \lambda_2 G_2\right) + \left(\frac{1}{Va} G_2 + \pi\sqrt{Ta} A_{11}\right) + \pi\sqrt{Ta}\lambda_1 G_1\right),\ D_3 = -\frac{Va}{\lambda_1}\left(\left(C_{20} + \lambda_2 G_3\right) + \frac{1}{Va} G_3\right)$

$G_4 = -\frac{1}{\gamma}\left(k\, f(z) A_{11} + \delta^2 B_{11} - Ra_I B_{11} + 2\pi k A_{11} B_{02}\right),\ D_4 = -\frac{1}{\gamma}\left(\left(4\pi^2 - Ra_I\right) B_{02} - \frac{\pi k}{2} A_{11} B_{11}\right)$

A competent numerical approach is advised for practical use as an alternative to analytically solving the aforesaid equations. Nonetheless, many qualitative conclusions may be drawn. Many crucial aspects of the whole issue are maintained by the homogeneously constrained time system (33). For $Ra_I < \left(\delta^2/2\right) + 2\pi^2$,There is a permanent negative divergence in the velocity field., i.e.,

$$\nabla \cdot \left(\frac{d\mathbf{X}}{dt}\right) = -\left(\frac{3}{\lambda_1}\left(Va\,\lambda_2 + 1\right) + \frac{1}{\gamma}\left(\delta^2 + 4\pi^2 - 2Ra_I\right)\right) \tag{34}$$

This shows that the system's behaviour is constrained, leading to trajectories in the phase space converging towards a fixed point with a small enough measure to be ignored. This causes the phase space volume to decrease with time. This idea is further shown by Eq. (35), which shows that if a collection of starting locations in space covers a volume $V(0)$ at t = 0, then after time t, the terminal points of their pathways will be constrained to an area of decreased volume.

$$V(t) = V(0)\exp\left(-\left(\frac{3}{\lambda_1}\left(Va\,\lambda_2 + 1\right) + \frac{1}{\gamma}\left(\delta^2 + 4\pi^2 - 2Ra_I\right)\right)t\right). \tag{35}$$

Larger values of the Vadasz number, strain-retardation number, and heat-capacity ratio are used to highlight the exponential decline in volume with time, whereas lower values of the Deborah number and heat-capacity ratio are used in contrast.

We are moving from qualitative to quantitative research by looking into the possibility of an analytical answer. Closed-form solutions of Eqs. (33) are derived for the stable case, allowing for effective analytical exploration of finite amplitude instability using the truncated model (Eq. From (33) we get the following formula by excluding all words except A_{11}

$$A_{11}\left(\left(\delta^2 + \pi^2\, Ta\right) - \left(k^2 Ra_D f(z) \Big/ \left(\left(\delta^2 - Ra_I\right) + \frac{2\pi^2 k^2}{\left(\pi^2 - Ra_I/4\right)}\left(\frac{A_{11}^2}{8}\right)\right)\right)\right) = 0 \tag{36}$$

The solution $A_{11} = 0$ symbolizes the pure conduction state. Thus, the second option guarantees the likelihood of finite amplitude steady convection, by offering the value of the finite-amplitude $A_{11}^2/8$ of convective motions, in the form.

$$\left(\frac{A_{11}^2}{8}\right) = \frac{\left(\pi^2 - Ra_I/4\right)}{2\pi^2 k^2}\left(\frac{k^2 Ra_D f(z)}{\left(\delta^2 + \pi^2\, Ta\right)} - \left(\delta^2 - Ra_I\right)\right) \tag{37}$$

Understanding the significance of the Rayleigh number necessitates going beyond just establishing the onset condition for convection, and instead looking at its effect on heat transfer. Therefore, it is crucial to the study of convection to quantify the heat flux across the layer. Because of the immobile nature of the initial state, heat can

only be transferred through conduction. But once the Rayleigh number is greater than a critical value, convection begins to develop. TheNusselt number is used to quantify the heat transferred by convection inside the layer:

$$Nu = 1 + \left(\int_0^{2\pi/k_c} \left(\partial T / \partial z \right) dx \Big/ \int_0^{2\pi/k_c} \left(\partial T_b / \partial z \right) dx \right)_{z=0}$$

By using (32b) and (12), one can obtain

$$Nu = 1 - 2\pi \left(\left(\tan \sqrt{Ra_I} \right) \Big/ \sqrt{Ra_I} \right) \left(B_{02} \right)_{z=0} \tag{38}$$

This on relieving the value of B_{02} at $z = 0$ delivers

$$Nu = 1 + \left(2\pi^2 k^2 \left(A_{11}^2 / 8 \right) \Big/ \left(\left(\pi^2 - Ra_I / 4 \right) \left(\delta^2 - Ra_I \right) + 2\pi^2 k^2 \left(A_{11}^2 / 8 \right) \right) \right) \tag{39}$$

Further, the values of $A_{11}^2/8$ and Ra_D^{St} computed respectively from (37) and (29) are substituted into (44) to obtain

$$Nu = 1 + \left(2\pi^4 k^2 \left(A_{11}^2 / 8 \right) \Big/ f(0) \left(\pi^2 - Ra_I / 4 \right)^2 \left(\delta^2 - Ra_I \right) \right) \left(Ra_D^{St} / Ra_D \right) \tag{40}$$

This approach becomes more meaningful for Darcy-Rayleigh numbers close to the critical value. Including additional terms in the Fourier expansion often leads to improved results. The unstable equations (33) are solved using the Runge-Kutta-Gill technique. The Nusselt number, *Nu*, is estimated as a function of time by computing the amplitudes for various time intervals.

5. RESULTS AND DISCUSSION

The primary objective of this investigation is to determine the critical Rayleigh number required to initiate convection. By precisely adjusting the parameters that influence the Rayleigh number, we can effectively control and manage the onset of convective motions. This study explores the combined impact of internal heat sources and rotation on the convection phenomenon. The relationship between the Rayleigh number and the wavenumber k is depicted in Figure 1.

The topologically connected neutral (marginal) stability curves in the (R_a, k) plans are shown in the plots. This connectedness allows us to express the linear stability criterion in terms of the Rayleigh number. The fluid becomes unstable above this curve, while it remains stable below it. Factors such as viscous relaxation, rotation, and internal heat generation shift the stability margins, thereby affecting the onset of convection. This confirms the ongoing relevance of the stability exchange concept. Since the threshold for oscillatory convection is significantly lower than that for stationary convection, the oscillatory mode is the preferred mechanism in this context.

Figure 1(b) shows that the stationary marginal curves rise with increasing Taylor number (Ta), highlighting the stabilizing effect of rotation. Conversely, for lower rotation rates, the oscillatory mode is affected differently. As Ta is further increased to significantly higher values, the system stabilizes towards the oscillatory onset, with Rac shifting to higher values. The Internal Rayleigh number (Ra_I) is a dimensionless parameter that quantifies the effect of heat produced by an internal source. The marginal stability curves for different variables are presented in Figure 1(c). The value of R_ac for both modes decrease as Ra_I increases, suggesting that even a small temperature gradient between the bounding surfaces can trigger convection due to internal heating. Additionally, the figure indicates that internal heating does not affect the critical wavenumber.

Figure 1(d) shows the effect of the Deborah number (De) on the onset threshold. Deborah number has no impact on stationary convection, but as De increases, the oscillatory neutral curves shift to lower levels. This means that higher values of De allow oscillatory convection to occur at a lower temperature gradient. The critical wavenumber remains unaffected by De.

Figure 1(e) illustrates the influence of the strain-retardation parameter (ϵ\epsilonϵ), which arises from viscoelasticity. Similar to the Deborah number, ϵ\epsilonϵ does not affect the stability boundary for stationary convection. However, higher values of ϵ\epsilonϵ significantly enhance Ra_c, indicating increased stability in the oscillatory mode. A close examination of the curves shows a minimal rise in the value of k_c.

Figure 1(f) depicts the impact of the heat-capacity ratio (β\betaβ). The stationary neutral curves are unaffected by β\betaβ, but the oscillatory convection curves shift to higher levels as β\betaβ increases. This implies that convection onset can be delayed by choosing a higher β\betaβ value. Additionally, the critical wavenumber shifts slightly upward, suggesting that while the size of convection cells remains largely unchanged, the heat-capacity ratio significantly impacts the onset of convection.

The point at which the neutral stability curve reaches its minimum represents the convection threshold. The detailed behavior of this critical value is examined as a function of the strain-retardation number (ϵ\epsilonϵ) in Figure 2, the Vadasz number (Va) in Figure 3, and the Taylor number (Ta) in Figure 4. It has been noted that the critical Rayleigh number (Rac) for stationary convection is independent of viscoelasticity and is much higher than that for oscillatory convection ($Rac,_{osc}$). This is illustrated by a dotted line in Figure 2(a), which remains at the highest level and unchanged for Rac and $Rac,_{osc}$. All the Ra _Rac-ϵ\epsilonϵ curves lie at a lower level, indicating that convection onset occurs through the oscillatory mode. The value of $Rac,_{osc}$ increases with ϵ\epsilonϵ, meaning the strain-retardation parameter enhances system stability, but this effect is mitigated by the internal Rayleigh number (RaI), as $Rac,_{osc}$ significantly decreases with increasing RaI. The influence of ϵ\epsilonϵ on $Rac,_{osc}$ is limited to a specific range of RaI; beyond this range, oscillatory convection ceases. Figure 2(b) shows the variation of $Rac,_{osc}$ with RaI. As IRaI increases, the stability curves for both stationary and oscillatory cases shift downward, confirming that internal heating promotes the onset of convection.

To explore the effect of varying the Vadasz number, we plot the critical curves in the Ra_c-Va plane for different values of β\betaβ in Figure 3. The Vadasz number (Va) has a dual nature. For smaller values of Va, $Rac,_{osc}$ decreases, a trend that continues up to a specific value of Va, beyond which the trend reverses. Therefore, although Va stabilizes the system towards the oscillatory mode, a slight destabilizing effect is observed for smaller Va values. This figure also shows that by selecting larger values for the specific heat ratio (β\betaβ), the value of $Rac,_{osc}$ can be increased, reinforcing the stabilizing influence of Va with β\betaβ.

In Figure 4, the impact of the Coriolis force, resulting from the rotation of the porous layer, is depicted through curves in the Ra_c-Ta plane. The critical Rayleigh number (Ra_c) increases exponentially with the Taylor number (Ta), indicating that increasing the rotation rate delays the onset of convection. The figure also shows that these critical curves shift downward as the strength of the internal heat source increases, meaning that the internal Rayleigh number (Ra_I) counteracts the stabilization effect of the Coriolis force.

After conducting a linear stability analysis to understand the convection threshold, a weak non-linear stability analysis was performed. This analysis helps measure the amplitude of convective motions and the extent of heat transfer, quantified by the Nusselt number (Nu). The influence of the Darcy-Rayleigh number on Nu is presented in Figures 5(a) and 5(b). At the onset, Nu is 1, but as the Darcy-Rayleigh number increases to about five times the critical Rayleigh number, Nu rises. Beyond this point, Nu becomes less sensitive to further increases. Therefore, in the vicinity of the convection onset, heat transfer enhancement occurs and is maintained even with further increases in the Darcy-Rayleigh number. Figure 5(a) shows that Nu increases with higher internal heat production, indicating that an internal heat source within the porous layer amplifies heat transport. Figure 5(b) examines the effect of rotation on the heat transfer coefficient, showing that Ta has no significant impact on Nu. Thus, despite the considerable role of rotation in system stabilization, it does not significantly affect the heat transfer variation.

The eighth-order Lorenz model was numerically solved using the Runge-Kutta-Gill method for the unstable finite-amplitude analysis. After computing the amplitudes as a function of time (t), these values were used to calculate Nu. The behavior of the heat transfer coefficient over time is graphically shown in Figures 6(a)-(f) as curves in the Nu,t plane. Initially, Nu is set to 1 (conduction). As time progresses, Nu fluctuates around an average value, indicating a transient pattern in the heat transfer coefficient. Eventually, Nu stabilizes, approaching the value expected for a stable finite-amplitude scenario.

In Figure 6(a), a significant increase in the heat transfer coefficient is observed when the Rayleigh number is three times its critical value. It also shows that Nu's sensitivity to time increases with higher internal heat production (Ra_I). Figure 6(b) demonstrates that heat transfer is enhanced with increasing Ra_I due to its destabilizing effect.

Figure 6(c) shows the influence of rotation, revealing that higher rotation rates cause greater fluctuations in Nu over time. However, at a specific point in time, Nu decreases with increasing Ta, confirming that the Coriolis force inhibits heat transfer.

Figures 6(d), 6(e), and 6(f) illustrate that convective heat transfer increases with the Vadasz number (Va), Deborah number (De), and heat capacity ratio (β\betaβ). Conversely, the strain-retardation parameter (ϵ\epsilonϵ) has a very minor impact on the heat transfer coefficient (this figure is not included for brevity).

6. CONCLUSIONS

The findings discussed above lead to the following conclusions:

- Viscoelasticity has minimal impact on stationary convection.
- Early onset of convection is influenced by the internal heat generation coefficient and stress-relaxation parameter.
- Rotation and heat-capacity ratio delay the onset of convection.
- Strain-retardation time reinforces stability in the oscillatory case.
- The range of values of the retardation parameter, within which oscillatory convection occurs, depends on the magnitude of the relaxation time. Beyond this range, oscillatory convection ceases, and instability is established through a stationary mode.
- The Vadasz number exhibits a dual effect on oscillatory convection.
- The heat transfer coefficient increases with increasing values of the Darcy-Rayleigh number, internal Rayleigh number, Vadasz number, Deborah number, and heat capacity ratio. Conversely, the trend reverses with increasing values of the Taylor number.
- Proper tuning of the governing parameters allows for either advancing or delaying convection, depending on the practical application.
- Some of the earlier results serve as special cases, providing strong validation for the findings of the current investigation.
- The present study can be extended to investigate sparsely packed porous layers, anisotropic porous layers saturated with Oldroyd-B fluid, and other types of non-Newtonian fluids to explore their stability properties.

Acknowledgement

The authors thank the Reviewers for their constructive remarks and useful suggestions, which improved the work significantly.

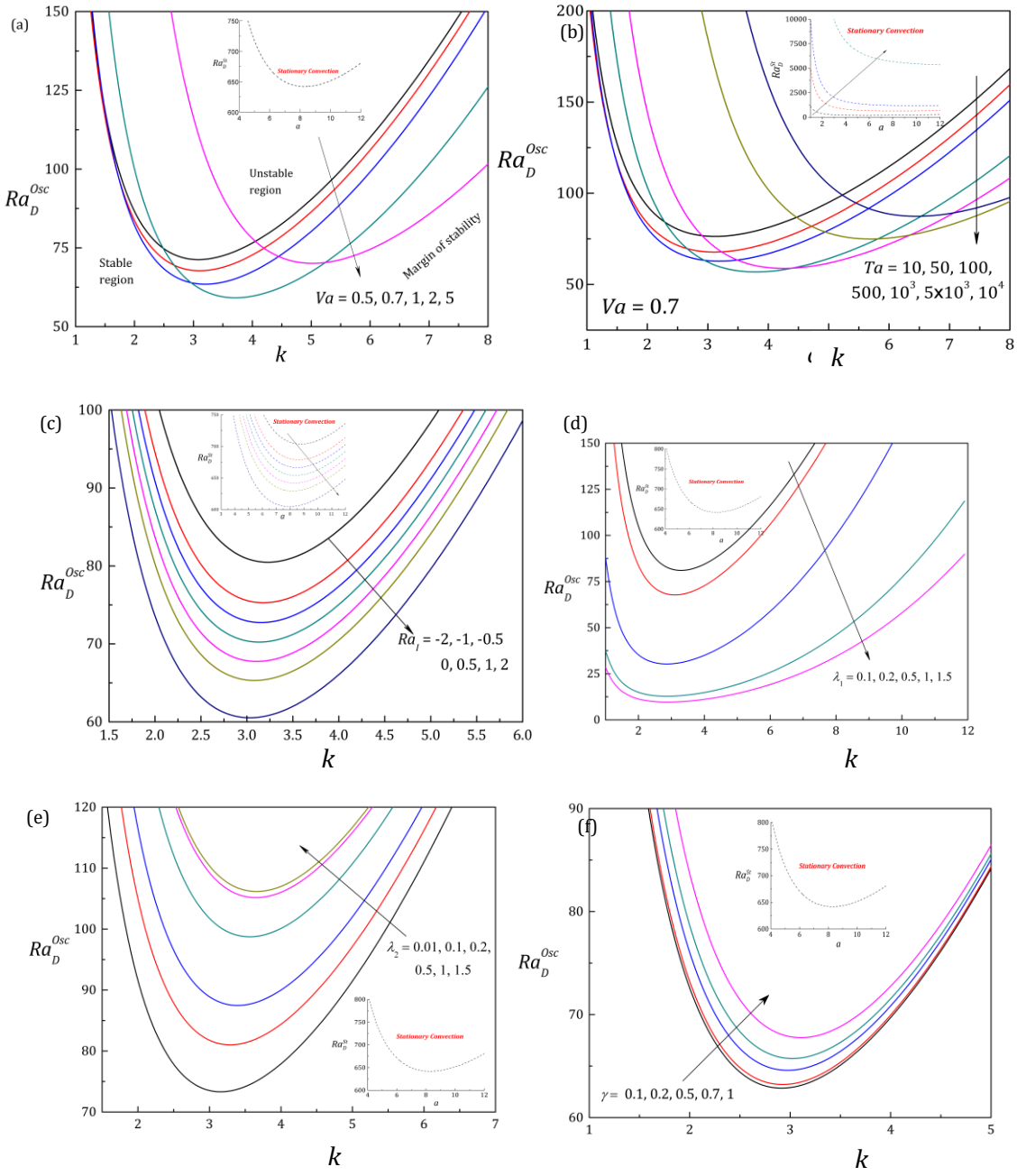

Figure 1.Neutral stability curves for different values of(a) Va, (b) Ta, (c) , (d) , (e) , (f)

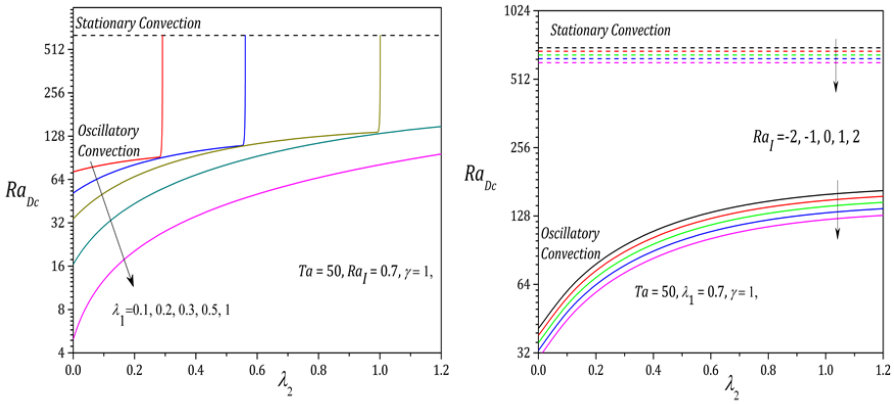

Figure 2.Variation of with for different values of(a) , (b)

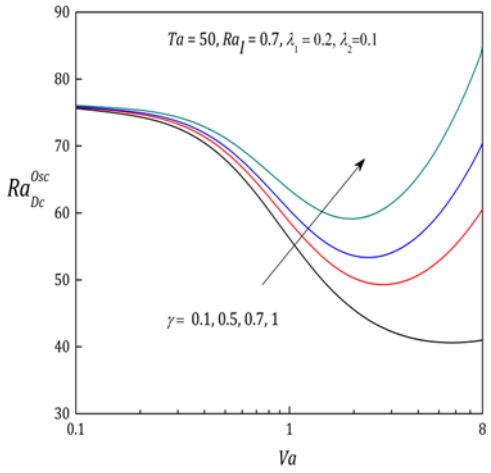

Figure 3.Variation of with for different values of

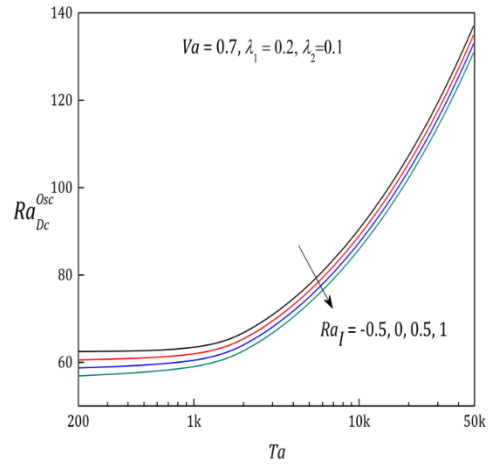

Figure 4.Variation of with for different values of

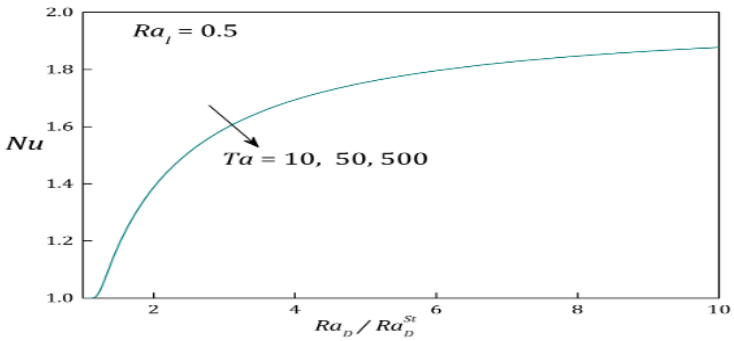

Figure 5.Variation of with for different values of(a) , (b) Ta

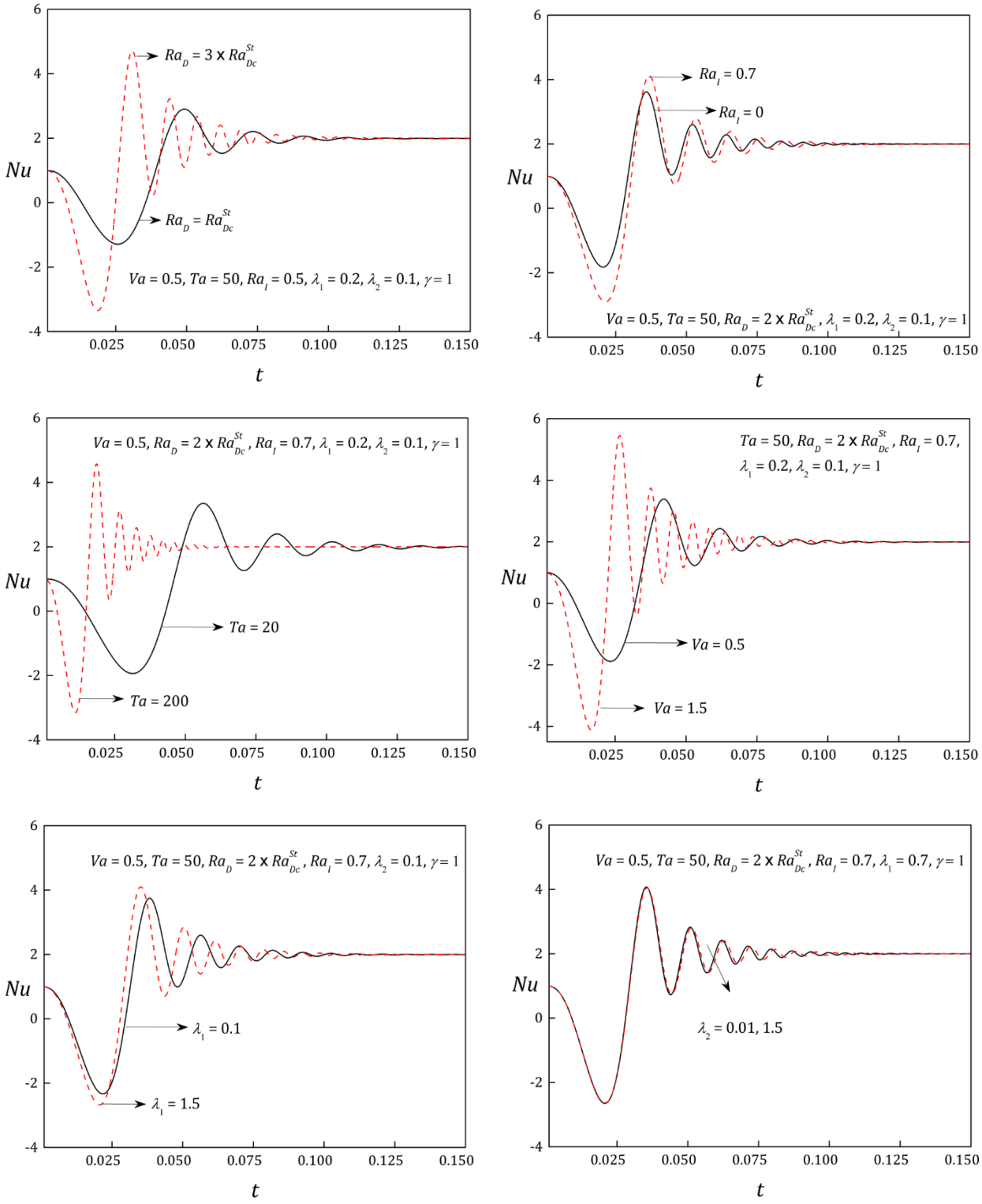

Figure 6. Variation of *Nu* with *t* for different values of (a) Ra_D, (b) Ra_I, (c) *Ta*, (d) *Va*, (e) and (f) γ

REFERENCES

[1] Ingham ,D.B, PopI. Transport Phenomena in Porous Media. Oxford: Pergamon; 1998.
[2] Ingham,D.B, PopI. Transport Phenomena in Porous Media-III. Oxford: Elsevier; 2005.
[3] Nield, D.A, BejanA. Convection in porous media, 3rd edn. New York: Springer; 2006.
[4] Vafai,K. Hand book of Porous Media. Boca Raton: Taylor and Francis (CRC); 2005.
[5] Vadasz, P. Emerging Topics in Heat and Mass Transfer in Porous Media. New York: Springer; 2008.

[6] Lowrie,W. Fundamentals of Geophysics. Cambridge: Cambridge University Press; 2020.
[7] LiZ, Khayat ,R.E. Finite-amplitude Rayleigh–Benard convection and pattern selection for viscoelastic fluids. J. Fluid Mech.2005; 529: 221–251.
[8] Kim ,M.C, Lee, S.B, Kim,S. Thermal instability of viscoelastic fluids in porous media. Int. J. Heat Mass Tra. 2003; 46: 5065–5072.
[9] O'ConnellRJ, Budiansky ,B. Viscoelastic properties of fluid saturated cracked solids. J. Geophys. Res. 1977; 82: 5719–5739.
[10] Griffiths ,RW. Effects of earth's rotation on convection in magma chambers. Earth Planet Sci. Lett.1987; 85: 525–536.
[11] Rudraiah,N., Kaloni ,P.N., Radhadevi,P.V. Oscillatory convection in a viscoelastic fluid through a porous layer heated from below. Rheol Acta. 1989; 28: 48-53.
[12] Yoon ,D.Y., Kim ,M.C., Choi,C .K. Onset of oscillatory convection in a horizontal porous layer saturated with viscoelastic liquid. Transport Porous Media. 2004; 55: 275-284.
[13] Malashetty ,M.S., Shivakumara ,I.S., Kulkarni ,S. Convective Instability of Oldroyd-B Fluid Saturated Porous Layer Heated from Below using a Thermal Non-equilibrium Model. Transport Porous Media. 2006; 62: 55-79.
[14] Swamy ,M.S., Naduvinamani,N.B., Sidram,W. Onset of Darcy-Brinkman convection in a binary viscoelastic fluid saturated porous layer. Transport Porous Media. 2012; 94: 339-357.
[15] Friedrich,R. Einflu der Prandtl-Zahl auf die Zellularkonvektion in einem rotierendenmit Fluid gesattigten porosen medium. Z. Angew. Math. Mech.1983; 63: 246–249.
[16] Patil,P.R., Vaidyanathan,G. On setting up of convective currents in a rotating porous medium under the influence of variable viscosity. Int. J. Eng. Sci.1983; 21: 123–130.
[17] Palm,E., Tyvand,A. Thermal convection in a rotating porous layer. Z. Angew. Math. Phys.1984; 35: 122–123.
[18] Jou,J.J, LiawJS. Thermal convection in a porous medium subject to transient heating and rotating. Int. J. Heat Mass Transfer. 1987; 30: 208–211.
[19] Qin,Y., Kaloni ,P.N. Nonlinear stability problem of a rotating porous layer. Quart. Appl. Math.1995; 0: 129–142.
[20] Vadasz,P. Coriolis effect on gravity-driven convection in a rotating porous layer heated from below. J. Fluid Mech.1998; 376: 351–375.
[21] Straughan,B. A sharp nonlinear stability threshold in rotating porous convection. Proc. Roy. Soc. Lond. A.2001; 457: 87–93.
[22] Govender,S. Oscillating convection induced by gravity and centrifugal forces in a rotating porous layer distant from the axis of rotation. Int. J. Eng. Sci.2003; 41: 539-545.
[23] Malashetty,M.S., Swamy,M. The effect of rotation on the onset of convection in a horizontal anisotropic porous layer. Int. J. Therm. Sci.2007; 46: 1023–1032.
[24] Malashetty,M.S,. Swamy,M.S. Effect of rotation on the onset of thermal convection in a sparsely packed porous layer using a thermal non-equilibrium model. Int. J. Heat Mass Transf.2010; 53: 3088–3101.
[25] Malashetty,M.S., Swamy,M.S., Effect of gravity modulation on the onset of thermal convection in rotating fluid and porous layer. Physics of Fluids. 2011; 0: 64108.
[26] Malashetty,M.S., Swamy,M.S, Sidram,W. Thermal convection in a rotating viscoelastic fluid saturated porous layer. Int. J. Heat Mass Transf.2010; 53: 5747-5756.
[27] Malashetty,M.S., Swamy,M., Kulkarni,S. Thermal convection in a rotating porous layer using a thermal nonequilibrium model. Physics of Fluids. 2007; 0: 54102.
[28] Capone,F., Luca,R.De, Gentile,M. Thermal convection in rotating anisotropic bidispersive porous layers. Mech. Res. Comm.2020; 110: 103601.
[29] Enagi,N.K., Chavaraddi ,K.B., Kulkarni,S. Effect of maximum density and internal heating on the stability of rotating fluid saturated porous layer using LTNE model. Heliyon. 2022; : e09620.
[30] Thirlby,R. Convection in an Internally Heated Layer. J. Fluid Mech.1970; 44: 673.
[31] Ahmed,S.E., Rashed ,Z.Z. MHD natural convection in a heat generating porous medium-filled wavy enclosures using Buongiorno's nanofluid model. Case Studies in Therm. Engng.2019; 14: 100430.
[32] Mahabaleshwar,U.S, Basavaraja,D., Wang,S. Convection in a porous medium with variable internal heat source and variable gravity. Int. J Heat Mass Transfer. 2017; 111: 651-656.